The American Journal of Chinese Medicine, Vol. 45, No. 4, 813–832

Institute for Advanced Research in Asian Science and Medicine
DOI: 10.1142/S0192415X17500434

The Effects of *Gymnema sylvestre* in High-Fat Diet-Induced Metabolic Disorders

Hyeon-Jeong Kim,[*] Sanghwa Kim,[*,†] Ah Young Lee,[*]
Yoonjeong Jang,[*] Orkhonselenge Davaadamdin,[*] Seong-Ho Hong,[*,‡]
Jun Sung Kim[§] and Myung-Haing Cho[*,†]

[*]*College of Veterinary Medicine, Seoul National University*
Gwanak-ro 1-gil, Gwanak-gu, Seoul 08826, Republic of Korea

[†]*Graduate Group of Tumor Biology, Seoul National University*
Daehangno 103-gil, Jongno-gu, Seoul 03080, Republic of Korea

[‡]*New Drug Development Center, Daegu-Gyeongbuk*
Medical Innovation Foundation, 88-gil, Dong-gu
Daegu 41061, Republic of Korea

[§]*R&D Center, Biterials Co., Ltd., Siksa-dong, Ilsandong-gu*
Goyang-si, Gyeonggi-do 10326, Republic of Korea

Published 18 May 2017

Abstract: This study used an integrated approach to investigate the effects of *Gymnema sylvestre* (GS) extract as a functional dietary supplement with a high-fat diet. This approach examined insulin resistance, the dysfunction of adipose tissue, and liver steatosis. Male C57BL/6J mice were fed a normal chow or high-fat diet (HFD) for the acute and chronic study, in addition to GS in different doses (100, 250 and 500 mg/kg body weight). Their body composition changes, serum lipid and glucose parameters, adipose and liver tissue histology, and gene expression were measured. It was found that GS significantly suppressed the increase of body weight, serum levels of lipid, insulin and leptin, and adipose tissue, and liver inflammation. GS also demonstrated hypoglycemic effects due to the amylase inhibition activity. Our results support the existence of a relationship between the HFD induced insulin resistance, adipose dysfunction and liver steatosis. In conclusion, GS works as a functional dietary supplement with preventative effects against metabolic disorder.

Keywords: Obesity; Diabetes; Adiposity; High-fat Diet; Hyperglycemia.

Correspondence to: Prof. Myung-Haing Cho and Dr. Jun Sung Kim, College of Veterinary Medicine, Seoul National University, Gwanak-ro 1-gil, Gwanak-gu, Seoul 08826, Republic of Korea. Tel: (+82) 2-880-1276, Fax: (+82) 2-873-1268, E-mail: mchotox@snu.ac.kr (M.-H. Cho); R&D Center, Biterials Co., Ltd., Siksa-dong, Ilsandong-gu, Goyang-si, Gyeonggi-do 10326, Republic of Korea. Tel: (+82) 2-792-3776, Fax: (+82) 2-792-3779, E-mail: lifeisgood@biterials.com (J.-S. Kim)

Introduction

Obesity is associated with various metabolic disorders such as insulin resistance, diabetes, hypertension, stroke, cardiovascular disease, and nonalcoholic fatty liver disease (NAFLD), (Pothuraju *et al.*, 2013; van der Heijden *et al.*, 2015). Among the numerous causes of obesity, nutrient overload due to an increased intake of a high-fat diet (HFD) is regarded as a prominent factor that causes an imbalance between energy intake and expenditure (Strauss *et al.*, 2000; Li *et al.*, 2013; Gao *et al.*, 2015). For this reason, HFD-induced obesity in rodents is considered a good model to study metabolic disorders including adiposity, hepatic lipid accumulation and insulin resistance (Bhutani *et al.*, 2007; Jin *et al.*, 2013; Tanaka *et al.*, 2015).

Over the last two decades, knowledge regarding obesity-induced insulin resistance has improved significantly; it has been found that the disorder is closely related to the pathogenesis of type 2 diabetes, adipocyte dysfunction and NAFLD (Begriche *et al.*, 2013). Dysfunction of adipose tissue causes metabolic disruption in energy homeostasis as well as an energy imbalance, and plays a role in NAFLD development and progression (Gastaldelli *et al.*, 2009; Duval *et al.*, 2010). In addition, chronic inflammation characterized by macrophage infiltration or excessive lipid accumulation in adipocytes contributes to hypertrophied adipocytes. The latter lead to changes in the secretion levels of adipokines such as adiponectin and leptin. These pathological conditions are strongly linked to insulin resistance in obesity (Lumeng and Saltiel, 2011; Jiang *et al.*, 2011).

As noted, the changed metabolic state of the liver depends on the rise of insulin resistance and the inflammation of adipose tissue. With these changes, the liver can gain hepatic dysfunction such as NAFLD. The liver is well known for its ability to regulate energy homeostasis and systemic metabolic balance. However, pro-inflammatory activation of Kuffer cells is induced by the consumption of a HFD, and can lead to obesity-induced liver disease and insulin resistance (Asai *et al.*, 2014; van der Heijden *et al.*, 2015). Thus, insulin resistance, adipose dysfunction and NAFLD are correlated with HFD-induced obesity (Asai *et al.*, 2014; García-Ruiz *et al.*, 2015).

At present, natural herbal resources with biological activities have been widely investigated as anti-obesity and antidiabetic agents. *Gymnema sylvestre* (GS) is a woody climber of the Asclepiadaceae family, and is mainly found in the tropical regions in the world (Leach, 2007). It is well known for its antihypercholesterolemia, anti-inflammatory and antimicrobial properties, in addition to its well-studied antidiabetic and anti-obesity effects (Vermaak *et al.*, 2011; Tiwari *et al.*, 2014; Kishore *et al.*, 2014). In many phytochemical analyses, GS is known to include gymnemic acids, stigmasterol, quercitol and amino acids derivative of betaine, ethylamine and choline. One of the major active compounds is gymnemic acids and found in all parts of the plant. This mechanism is known to stimulate insulin secretion from the pancreas and to delay the absorption of glucose into the blood. In addition, other compounds also have a similar effect; however, they have less pervasive antisweet effects than gymnemic acids do (Tiwari *et al.*, 2014; Kishore *et al.*, 2014).

In previous studies, the administration of GS (120 mg/kg/day) for seven days in streptozotocin (STZ)-treated diabetic mice increased the regeneration and function of

β-cells in pancreatic islets, resulting in higher serum levels of C-peptide (Shanmugasundaram *et al.*, 1990). Oral administration of GS also decreased the levels of blood glucose, glycated hemoglobin, and free fatty acid, while increasing insulin levels in STZ-treated diabetic rats (Daisy *et al.*, 2009; Kosaraju *et al.*, 2014). In addition, GS exhibited anti-obesity effects through decreased body weight gain and the serum levels of total cholesterol (TC), triglycerides (TG) and low-density lipoprotein (LDL)-cholesterol, (Shigematsu *et al.*, 2001; Reddy *et al.*, 2012; Kumar *et al.*, 2013). Many scientific studies involving GS, however, have been performed using mutant mice or rats such as *db/db*, *ob/db*, and STZ-treated diabetic models, and have not used oral administration.

In our previous studies, we made a mixed-feed containing HFD and GS that was used for 4 weeks. GS showed significant anti-obesity effects in comparison to only a HFD, but the hypoglycemic effect was insufficient (Kim *et al.*, 2016). Therefore, the objective of this study is to evaluate the acute and chronic antiobesity and antidiabetic effects of GS using correlated analyses of insulin resistance and the dysfunction of adipose tissue and the liver.

Materials and Methods

Extraction and Phytochemical Analysis of GS

The extract of GS was obtained from TC, TG, LDL-cholestrol in powder form and stored at 4°C until usage. To identify the amount of gymnemic acid in GS, HPLC and gravimetric analysis were performed. Extraction and HPLC were performed based on previous methods (Kusum *et al.*, 2014). The HPLC chromatogram for deacyl gymnemic acid is shown in Fig. S1, and the profile is described in Table S1.

Animal Experiments

Male C57BL/6J mice were purchased from Central Lab Animal Co. (Seoul, Korea), and housed under a 12-h dark/light cycle. All animal experiments were performed in accordance with the Seoul National University Animal Ethics Committee protocol (SNU-150829-3). After one week of acclimation on a normal chow (D12450K; Research Diets, New Brunswick, NJ, USA), animals were randomly divided. First, for acute study, mice were divided into 4 groups ($n = 5$, 7 weeks old): (i) a control (CON) group that received water, and three groups that received a single oral administration of GS, (ii) at 100 mg/kg body weight, (iii) at 250 mg/kg body weight and (iv) at 500 mg/kg body weight. Animals fed a normal chow in this experiment. Second, to evaluate the chronic effects, mice were divided into 5 groups ($n = 10$, 7 weeks old): (i) a control (CON) group fed a normal chow, (ii) a HFD group, a group fed a HFD plus GS, (iii) at 100 mg/kg body weight (HFD+GS 100 mg/kg group), (iv) at 250 mg/kg body weight (HFD+GS 250 mg/kg group) and (v) at 500 mg/kg body weight (HFD+GS 500 mg/kg group). The HFD contained 60% kcal fat (D12492; Research Diets), and all groups were fed the diet for 8 weeks. The detailed dietary composition is shown in Table S2. Body weight and food intake were assessed twice per week during the experimental period. Based on these measurements,

food efficiency ratio (increased body weight (g)/food intake (g)) and energy efficiency ratio (increased body weight (g)/energy intake (kcal)) were calculated.

Biochemical Analysis

Serum TC, TG, creatine, total protein, aspartate aminotransferase (AST), and alanine transaminase (ALT) levels were analyzed by the Preclinical Research Center (ChemOn, Inc., Gyeonggi-do, Korea). High-density lipoprotein (HDL)-cholesterol, LDL/very low-density lipoprotein (VLDL)-cholesterol, leptin, insulin, HbA1c, liver TG were measured with a commercial ELISA kit. Amylase activity was measured measured by serum after acute study of GS. All procedures were performed following the manufacturer's instructions.

Histological Analysis

The adipose tissues and liver samples were fixed in 10% neutral buffered formalin, paraffin processed, and sectioned at 5 μm. Paraffin-embedded sections were stained with hematoxylin and eosin (H&E) and Picrosirius Red according to the manufacturer's protocols, and then examined under a light microscope (Nikon Eclipse Ti; Nikon, Tokyo, Japan). The number and size of adipocytes and collagen deposition in the liver tissue were measured by using Image J Software (version 1.48; National Institutes of Health, Bethesda, MD, USA). The NAFLD activity score (NAS) data were analyzed based on the following histologic data: diagnosis rendered by the Pathology Committee (i.e. "not steatohepatitis", "borderline, zone 3 pattern", "definite steatohepatitis"); the aggregate NAS; the score of each component of the NAS (steatosis (0–3), lobular inflammation (0–3), ballooning (0–2)), and fibrosis scores (0,1a,1b,1c,2,3).

Oil Red O Staining

Liver tissues were fixed in 4% paraformaldehyde solution at 4°C for one day, transferred to 10%, 20%, and 30% sucrose solutions for one day each, and then embedded with Tissue-Tek OCT (Sakura, Torrance, CA, USA). The tissues were sectioned at 8 μm and stained with 0.5% Oil red O stock solution in propylene glycol (O1516, Sigma-Aldrich) for 10 min at 56°C, and then counterstained with Mayer's hematoxylin.

Glucose and Insulin Tolerance Tests

The intraperitoneal glucose tolerance test (IPGTT) and insulin tolerance test (ITT) were performed. For IPGTT, animals were fasted overnight and 1.5 g/kg body weight of glucose was administered by intraperitoneal injection. Using intraperitoneal injection, an ITT was performed after fasting for 6 h, using human insulin HI-0310 (Lilly, Indianapolis, USA) at a body weight of 0.75 U/kg. At the time points indicated, blood glucose concentrations were measured with an Accu-Chek glucometer (Roche, Basel, Switzerland).

Postprandial Glucose Test for Acute Study of GS

The postprandial glucose test was performed after a single oral administration of GS. Animals were put into a postprandial state with an intraperitoneal injection of glucose (1.5 g/kg body weight), and then a single oral administration of GS (100, 250, 500 mg/kg body weight) was performed after 10 min. At the time points indicated, blood glucose concentrations were measured.

Western Blotting

Western blotting was performed based on previous methods (Yu *et al.*, 2016), and membranes were immunoblotted with primary antibodies, specifically α-SMA (ab5694), UCP1 (ab10983) antibodies (Abcam, Cambridge, MA, USA), AMPKα (#2532) and pAMPKα (#2535) antibodies (Cell Signaling, Danvers, MA, USA), NF-κB (sc-372), p38 (sc-7942) and ß-actin (sc-1616HRP) antibodies (Santa Cruz Biotechnology, CA, USA). Secondary antibodies were conjugated to horseradish peroxide for 2 h at room temperature, rinsed and detected using an ATTO CS image analyzer 3.0 (ATTO, Tokyo, Japan).

RNA isolation and Real Time Quantitative Polymerase Chain Reaction

Total RNA was extracted by using the QuickGene RNA tissue kit SII (Fujifilm, Tokyo, Japan), and cDNA was synthesized with the Suprime script RT premix (GeNet Bio, Daejeon, Korea), according to the manufacturer's instructions. Quantitative Polymerase Chain Reaction was performed with the CFX96 real time system (Bio-Rad, Hercules, CA), and each cDNA was amplified with the Q-master mix (Genet Bio, Daejeon, Korea). The designed primers are shown in Table S3. We used Manager Version 2.1 Software (Bio-Rad) to analyze the data.

Immunohistochemistry

Primary F4/80 antibody (PA5-32399, Thermo Fisher Scientific) and UCP-1 (ab10983, Abcam) were used for immunohistochemistry (IHC) and performed according to the previous method (Yu *et al.*, 2016). The slides were observed using a light microscope (Eclips Ti-S, Nikon, Tokyo, Japan). Counting the number of positive cells and measuring intensity in randomly selected field images were performed using the Image J Software (Version 1.48; National Institutes of Health).

Statistical Analyses

Results are shown as the mean ± SEM. One-way analysis of variance (ANOVA) with a post hoc Student-Newman-Keuls multiple comparison test was performed using GraphPad (San Diego, CA, USA). IPGTT, ITT and a postprandial glucose tests were

statistically compared using a two-way repeated-measures ANOVA with a Bonferroni post hoc test (GraphPad). All results were considered statistically significant at $p < 0.05$.

Results

Effects of GS on Body Composition

The characteristics of the mice were determined in Table 1. The total body weight gain showed significant increases with a HFD, whereas GS significantly reduced the weight gain. Food intake decreased in the HFD+GS 500 mg/kg group, but this was due to bitter taste of GS. Food and energy efficiency ratios were significantly decreased in all concentrations of GS. Increased organ weight in the liver and white adipose tissue was also closely related to body weight gain, and the HFD group showed significant increases in the organ weight whereas these values were significantly decreased in the GS groups. These results suggest that the consumption of GS influenced the body weight gain induced by a HFD and led to a decreased food and energy efficiency ratio.

Table 1. Characteristics of Mice After 8-week Experimental Period

			HFD+GS(mg/kg)		
	CON	**HFD**	**100**	**250**	**500**
Initial BW (g)	25.38 ± 0.42	26.08 ± 0.44	24.85 ± 0.28	24.63 ± 0.53	24.88 ± 0.35
Final BW (g)	31.60 ± 0.57	$41.79 \pm 1.70^{***}$	$37.49 \pm 1.08^{**,\dagger\dagger}$	$37.45 \pm 0.66^{**,\dagger}$	$37.35 \pm 1.09^{***,\dagger}$
ΔBW (g)	6.22 ± 0.24	$15.72 \pm 1.29^{***}$	$12.64 \pm 0.82^{***,\dagger}$	$12.83 \pm 0.15^{***,\dagger}$	$12.47 \pm 0.75^{***,\dagger}$
Food intake (kcal/day/mouse)	13.76 ± 1.53	$16.54 \pm 1.29^{**}$	15.56 ± 2.06	15.65 ± 0.99	$14.77 \pm 1.35^{\dagger\dagger}$
Total energy intake (kcal)	780.35 ± 95.60	893.48 ± 105.35	882.73 ± 126.77	876.51 ± 55.33	853.22 ± 101.92
Food efficiency (%)	3.11 ± 0.25	$9.66 \pm 2.65^{***}$	$7.23 \pm 0.88^{***,\dagger\dagger}$	$7.32 \pm 0.32^{***,\dagger}$	$7.32 \pm 1.72^{***,\dagger}$
Energy efficiency (mg/kcal)	7.70 ± 1.00	$18.75 \pm 3.35^{***}$	$12.55 \pm 4.85^{***,\dagger}$	$14.10 \pm 1.00^{***,\dagger\dagger}$	$13.95 \pm 3.25^{***,\dagger\dagger}$
Organ weight					
Liver weight (g)	1.03 ± 0.01	$1.45 \pm 0.03^{***}$	$1.29 \pm 0.03^{***,\dagger\dagger\dagger}$	$1.27 \pm 0.04^{***,\dagger\dagger\dagger}$	$1.32 \pm 0.02^{***,\dagger\dagger}$
Epididymal fat weight (g)	0.79 ± 0.23	$3.49 \pm 0.67^{***}$	$2.80 \pm 0.45^{***,\dagger\dagger}$	$2.59 \pm 0.44^{***,\dagger\dagger\dagger}$	$2.54 \pm 0.48^{***,\dagger\dagger\dagger}$
Peritoneal fat weight (g)	0.41 ± 0.12	$1.18 \pm 0.14^{***}$	$1.09 \pm 0.15^{***,\dagger\dagger}$	$1.03 \pm 0.18^{***,\dagger\dagger}$	$1.03 \pm 0.17^{***,\dagger}$
Abdominal fat weight (g/g BW)	3.39 ± 0.82	$10.82 \pm 1.46^{***}$	$10.13 \pm 2.54^{***}$	$9.20 \pm 1.59^{***,\dagger}$	$10.00 \pm 2.30^{***,\dagger}$

Notes: All values are mean ± SEM. ($n = 8-10$) $^{**}p < 0.01$, $^{***}p < 0.001$ versus control (CON) group, $^{\dagger}p < 0.05$, $^{\dagger\dagger}p < 0.01$, $^{\dagger\dagger\dagger}p < 0.001$ versus high-fat diet (HFD) group.

Effects of GS on Glucose Homeostasis and Insulin Resistance

All HFD+GS groups showed significant decreases in the level of final fasting glucose, serum insulin, HOMA-IR and glycated hemoglobin (HbA1c) in the HFD group (Table 2). To further examine metabolic changes, we performed an IPGTT and ITT, finding that GS induced significantly lower glucose levels, as confirmed by the area under the curve (Figs. 1A and 1B). Additionally, to measure whether the single oral administration of GS also affects hyperglycemia, a postprandial glucose test and ITT were performed. At all concentrations of GS, glucose levels were significantly decreased relative to the CON group, as can be seen at 30, 60 and 90 min time marks (Fig. 1C). ITT also showed significant decreases at 60, 90 and 120 min in comparison to the CON group, as confirmed by the AUC (Fig. 1D). In addition, GS significantly reduced amylase activity at all concentrations (Fig. 1E). These results indicated that GS could ameliorate glucose intolerance and insulin resistance, decreasing postprandial glucose level by inhibiting amylase activity.

Effect of GS on Serum Levels of Lipid Parameters

The consumption of a HFD for 8 weeks induced marked elevation of serum TC, TG, LDL/VLDL-cholesterol, total protein and creatine, but also reduced HDL-cholesterol levels (Table 3). However, GS significantly decreased serum TC, TG, LDL/VLDL-cholesterol levels in comparison to the HFD group. In comparison to the CON group, the serum HDL-cholesterol level was significantly decreased in the HFD and HFD+GS 100 mg/kg groups, however, there were no significant changes in other groups. Serum creatine levels showed no significant differences among all groups.

Table 2. Effect of GS on the Glucose Homeostasis and Insulin Resistance

			HFD+GS(mg/kg)		
	CON	**HFD**	**100**	**250**	**500**
Initial fasting glucose (mg/dl, 0wk)	85.56 ± 1.94	85.30 ± 2.07	86.50 ± 1.70	86.80 ± 2.18	85.50 ± 1.55
Final fasting glucose (mg/dl, 8wk)	81.88 ± 0.98	$139.17 \pm 11.33^{***}$	$114.00 \pm 4.62^{**,\dagger}$	$108.86 \pm 3.56^{**,\dagger\dagger}$	$112.86 \pm 5.30^{**,\dagger}$
Serum insulin (ng/ml)	0.11 ± 0.01	$0.18 \pm 0.02^{*}$	$0.13 \pm 0.02^{*}$	$0.10 \pm 0.01^{\dagger}$	$0.11 \pm 0.01^{\dagger}$
HOMA-IR[1)]	0.59 ± 0.06	$1.77 \pm 0.30^{**}$	$0.93 \pm 0.17^{\dagger\dagger}$	$0.70 \pm 0.11^{\dagger\dagger}$	$0.72 \pm 0.11^{\dagger\dagger}$
Insulin sensitivity[2)]	1.74 ± 0.17	$0.60 \pm 0.10^{*}$	1.19 ± 0.23	$1.55 \pm 0.25^{\dagger}$	$1.47 \pm 0.19^{\dagger}$
HbA1c (%)	3.66 ± 0.13	$4.80 \pm 0.38^{*}$	4.12 ± 0.22	4.16 ± 0.08	$3.87 \pm 0.12^{\dagger}$

Notes: All values are mean $\pm$ SEM ($n = 5-7$). $^{*}p < 0.05$, $^{**}p < 0.01$, $^{***}p < 0.001$ versus control (CON) group, $^{\dagger}p < 0.05$, $^{\dagger\dagger}p < 0.01$ versus high-fat diet (HFD) group.

(i) HOMA-IR was calculated as follows: glucose (mmol/L) $\times$ fasting insulin (μIU/mL)/22.5.

(ii) Insulin sensitivity was calculated as follows: 1/HOMA-IR.

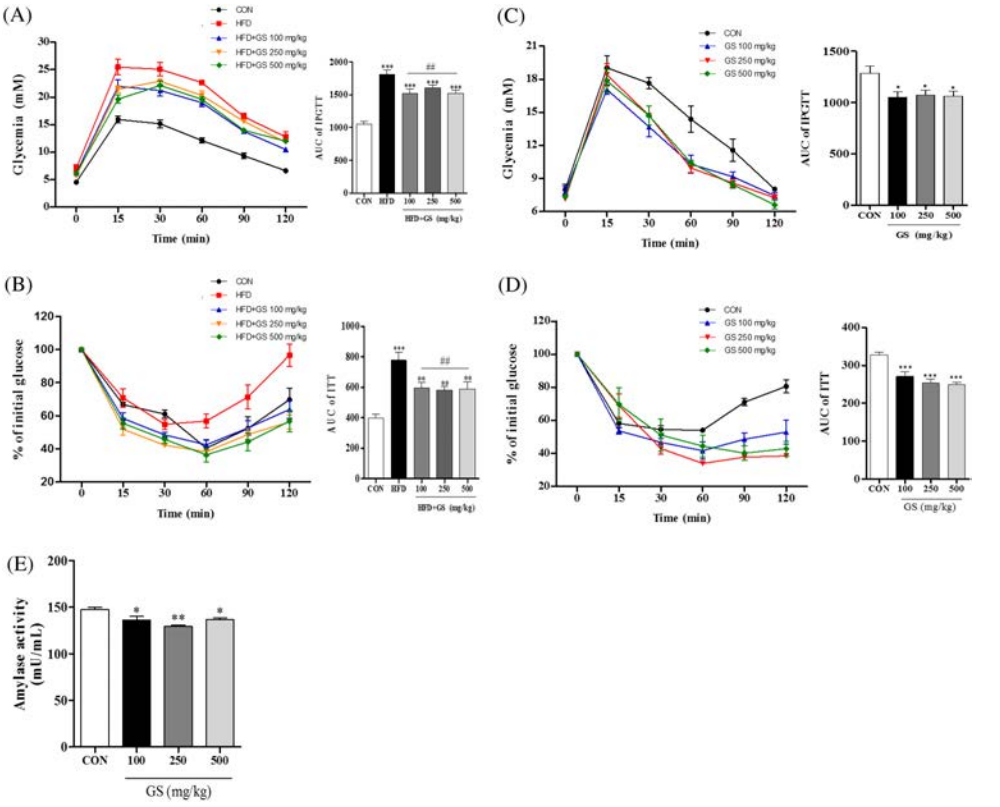

Figure 1. Effects of *Gymnema sylvestre* extract on glucose intolerance and insulin resistance. (A) Intraperitoneal glucose tolerance test (IPGTT) after 8 weeks and the area under the curve (AUC), (B) insulin tolerance test (ITT) after 8 weeks and the AUC, (C) postprandial glucose levels after single oral administration in normal C57BL/6J mice and the AUC, (D) insulin tolerance test (ITT) after single oral administration in normal C57BL/6J mice and the AUC and (E) amylase activity. Values are mean ± SEM. $^{*}p < 0.05$, $^{**}p < 0.01$, $^{***}p < 0.001$ versus control (CON) group, $^{\#}p < 0.05$, $^{\#\#}p < 0.01$ versus high-fat diet (HFD) group.

Effects of GS on Adiposity and Inflammation in White Adipose Tissue

Next, we questioned whether the previously beneficial effects of GS were related to adipose tissue. To test this, H&E staining and F4/80 IHC were performed (Fig. 2A). GS significantly increased the cell density (Fig. 2B), and the adipocyte mean area also significantly increased in comparison to the HFD group (Fig. 2C). The cells positive for F4/80 exhibited crown-like structures in the white adipose tissue (black arrow; Fig. 2A). An HFD induced a significant increase in macrophage (F4/80^{+}) infiltration relative to the CON group, however, GS significantly reduced it (Fig. 2D). GS also effectively decreased NF-κB and p38 protein levels (Fig. 2E) and the mRNA expression of TNF-α and SREBP-1c in comparison

Table 3. Serum Levels of Lipid

			HFD+GS(mg/kg)		
	CON	**HFD**	**100**	**250**	**500**
TC (mg/dl)	67.00 ± 3.00	$142.00 \pm 2.00^{***}$	$121.00 \pm 11.00^{***,\dagger}$	$107.00 \pm 23.00^{***,\dagger}$	$122.00 \pm 20.00^{***}$
TG (mg/dl)	41.00 ± 7.00	$62.00 \pm 20.00^{**}$	$41.00 \pm 9.00^{\dagger\dagger}$	$40.00 \pm 10.00^{\dagger\dagger}$	$48.00 \pm 14.00^{\dagger\dagger}$
HDL-cholesterol (mg/dl)	33.20 ± 10.22	$15.49 \pm 7.04^{*}$	$15.94 \pm 7.04^{*}$	19.12 ± 10.67	24.57 ± 7.95
LDL/VLDL-cholesterol (mg/dl)	4.36 ± 1.36	$19.58 \pm 6.13^{***}$	$18.21 \pm 7.95^{**}$	$10.27 \pm 2.27^{\dagger}$	$10.04 \pm 2.50^{\dagger}$
Creatine (mg/dl)	0.33 ± 0.02	0.34 ± 0.04	0.33 ± 0.03	0.30 ± 0.02	0.34 ± 0.00
Total protein (g/dl)	4.09 ± 0.30	$4.71 \pm 0.23^{**}$	$4.62 \pm 0.34^{*}$	4.31 ± 0.31	$4.45 \pm 0.29^{*}$

Notes: All values are mean $\pm$ SEM ($n = 5-7$). $^{*}p < 0.05$, $^{**}p < 0.01$, $^{***}p < 0.001$ versus control (CON) group, $^{\dagger}p < 0.05$, $^{\dagger\dagger}p < 0.01$, $^{\dagger\dagger\dagger}p < 0.001$ versus high-fat diet (HFD) group.

to the HFD group (Fig. 2F). Therefore, these results indicated that GS could prevent the adiposity and inflammation that is induced with the consumption of a HFD.

Effects of GS on Energy Homeostasis in White and Brown Adipose Tissue

To evaluate whether GS can regulate systemic energy homeostasis, UCP-1 IHC was performed in white and brown adipose tissue (Fig. 3A). In white adipose tissue, the expression level in the HFD+GS 250 mg/kg group was significantly higher in comparison to the HFD and HFD+GS 100 mg/kg groups (Fig. 3B). In addition, GS showed an increase in the protein levels of UCP-1 in white adipose tissue in contrast to significantly decreased protein levels in brown adipose tissue (Fig. 3C). With reduced the serum leptin levels (Fig. 3D), the mRNA expression of leptin and adiponectin also showed significant effects in white adipose tissue (Fig. 3E). These results suggest that GS could ameliorate energy imbalance by regulating leptin and adiponectin levels in white adipose tissue.

Effects of GS on Lipid Accumulation in the Liver

After feeding on a HFD for 8 weeks, microvesicular steatosis and inflammatory cell infiltration were observed with H&E and oil red O staining of liver slides (Fig. 4A). In the histopathological examination, GS showed significantly lower scores (Fig. 4B), especially with steatosis (Fig. 4C). With the changes of oil red O staining among the groups, the amount of neutral lipids in the liver was also significantly elevated in the HFD group as opposed to the GS-induced reduction (Fig. 4D). In addition, GS significantly elevated the ratio of phosphorylation of AMPKα (Fig. 4E). The activities of the liver marker enzymes, AST and ALT, were also significantly decreased (Figs. 4F and 4G). Consequently, these

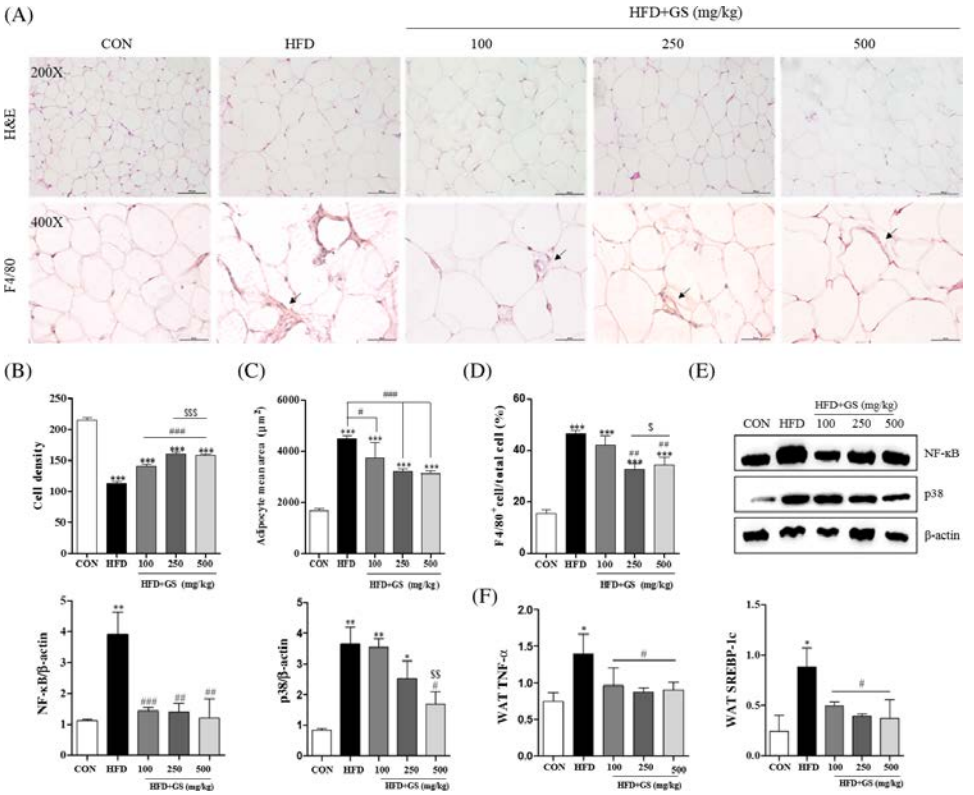

Figure 2. Effects of *Gymnema sylvestre* extract on adiposity and inflammation in white adipose tissue. (A) White adipose tissue stained with H&E and F4/80 IHC (black arrow: macrophage infiltration), (B) adipocyte density, (C) adipocyte mean area, (D) quantitative assessment of F4/80-positive cells per total cell, (E) relative protein levels of NF-κB, p38 and β-actin by western blot and densitometry, and (F) mRNA expression levels of TNF-α and SREBP-1c by qRT-PCR. Scale bars = 50 μm. Values are mean ± SEM. $^{*}p < 0.05$, $^{**}p < 0.01$, $^{***}p < 0.001$ versus control (CON) group, $^{\#}p < 0.05$, $^{\#\#}p < 0.01$, $^{\#\#\#}p < 0.001$ versus high-fat diet (HFD) group, $^{\$}p < 0.05$, $^{\$\$}p < 0.01$, $^{\$\$\$}p < 0.001$ versus high-fat diet containing GS 100 mg/kg body weight (HFD+GS 100 mg/kg) group.

results indicated that HFD triggered hepatic steatosis, but GS was able to significantly ameliorate these effects.

Effects of GS on Hepatic Inflammation and Fibrosis

We confirmed that HFD induced hepatic steatosis through collagen deposition and inflammation in the liver. Hepatic collagen deposition was evaluated with Sirius red staining (Fig. 5A) and the intensity was quantified (Fig. 5B). Macrophages in the liver were

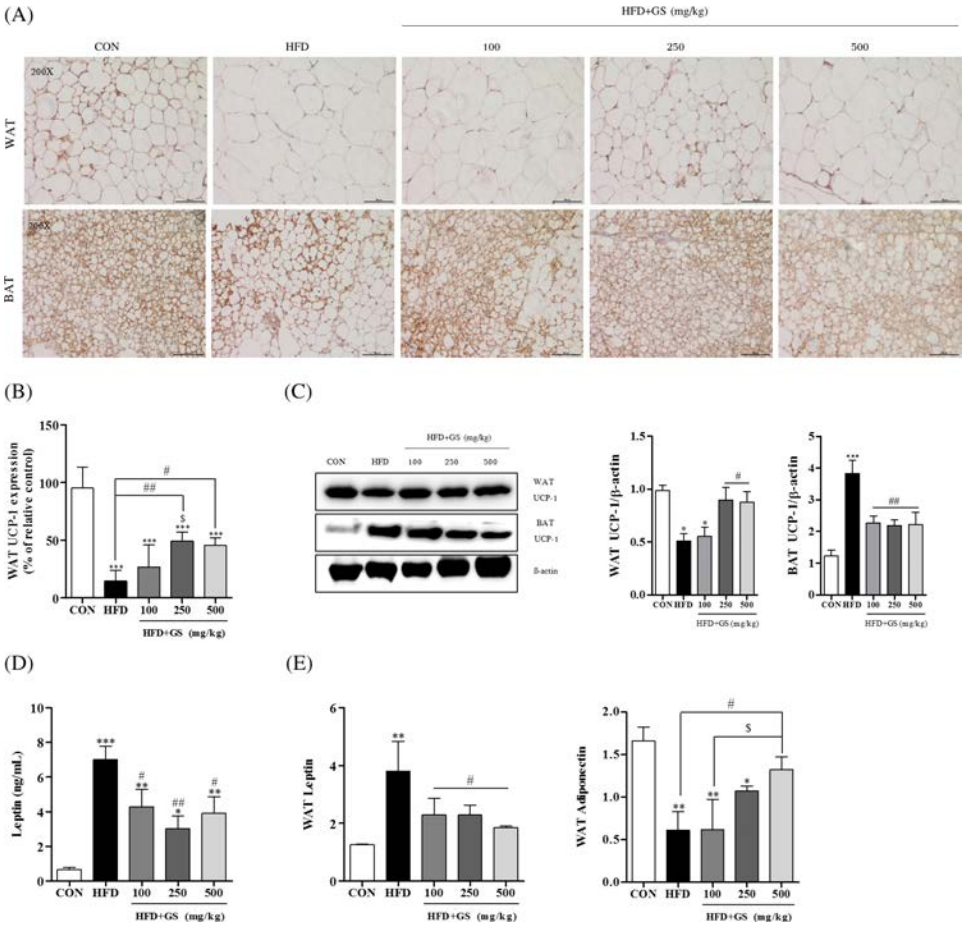

Figure 3. Effects of *Gymnema sylvestre* extract on energy homeostasis in white and brown adipose tissue. (A) IHC of UCP-1 in white and brown adipose tissue, (B) quantitative assessment of UCP-1-positive expression in white adipose tissue and (C) relative protein levels UCP-1 and β-actin in white and brown adipose tissue by Western blot and densutimetry, (D) serum leptin levels and (E) mRNA expression levels of leptin and adiponectin in white adipose tissue. Scale bars= 100 μm. Values are mean ± SEM. $^{*}p < 0.05$, $^{**}p < 0.01$, $^{***}p < 0.001$ versus control (CON) group, $^{\#}p < 0.05$, $^{\#\#}p < 0.01$ versus high-fat diet (HFD) group, $^{\$}p < 0.05$ versus high-fat diet containing GS 100 mg/kg body weight (HFD+GS 100 mg/kg) group.

identified by F4/80 IHC (Fig. 5A) and the percent area was quantified (Fig. 5C). In comparison to the CON group, the HFD group showed significant increases, while GS showed significant decreases. Additionally, GS significantly decreased the protein levels of α-SMA, NF-κB and p38 (Fig. 5E) as well as mRNA levels of TNF-α, TGF-ß, IL-6 and FAS (Fig. 5F). These results indicated that GS could ameliorate liver inflammation and fibrosis.

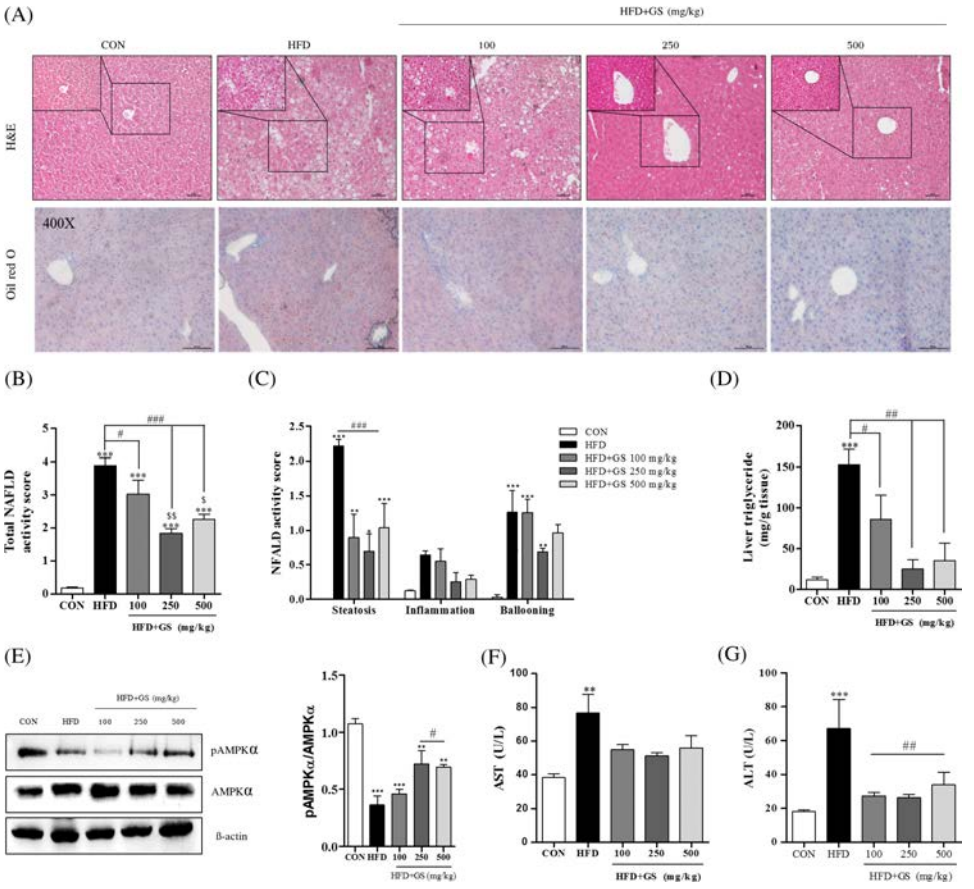

Figure 4. Effects of *Gymnema sylvestre* extract on lipid accumulation in the liver. (A) Liver tissue stained with H&E and oil-red O, (B) the non-alcoholic fatty liver disease (NAFLD) score, (C) separate scores for steatosis, inflammation and ballooning, (D) total liver TG content after 8 weeks, (E) relative protein levels of pAMPKα, AMPKα and β-actin by Western blot and densitometry, (F) serum AST level and (G) serum ALT level. Scale bars = 100 μm. Values are mean ± SEM. $^{*}p < 0.05$, $^{**}p < 0.01$, $^{***}p < 0.001$ versus control (CON) group, $^{\#}p < 0.05$, $^{\#\#}p < 0.01$, $^{\#\#\#}p < 0.001$ versus high-fat diet (HFD) group.

Discussion

The aim of this study is to investigate the anti-obesity and antidiabetic effects of GS as a functional dietary supplement in cases of a HFD. Many metabolic disorders induced by HFD are mainly related with insulin resistance, dysfunction of adipose tissue and liver. Our present study focused on these correlations and identified the potential and effectiveness of GS as a functional dietary supplement.

To study metabolic disorders caused by HFD, it is crucial to analyze the body composition (body weight gain, food and energy efficiency ratios and organ weight) and serum

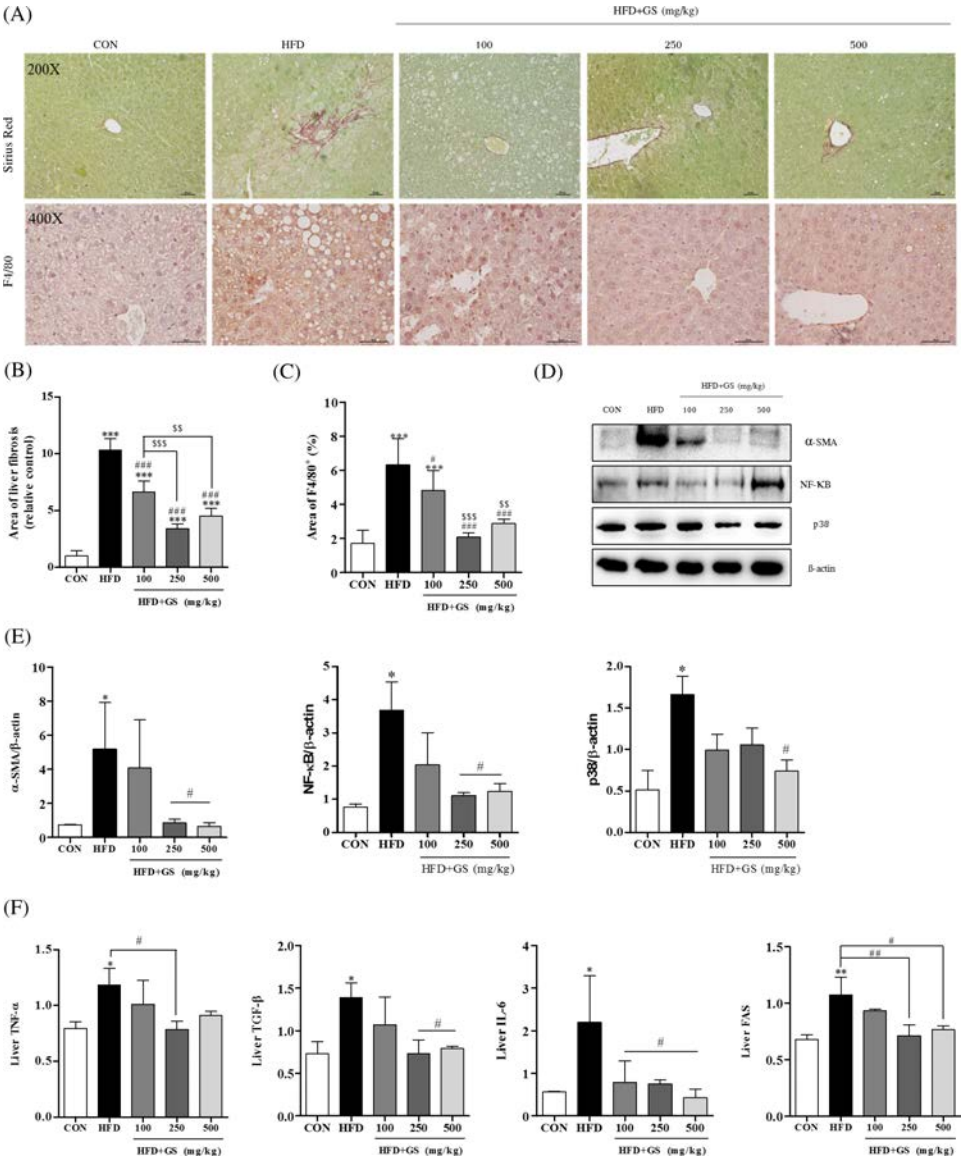

Figure 5. Effects of *Gymnema sylvestre* extract on hepatic inflammation and fibrosis. (A) Liver tissue stained with Sirius red and F4/80 IHC, (B) intensity of Sirius red, (C) intensity of F4/80 IHC, (D) relative protein levels of α-SMA, NF-κB, p38 and β-actin by Western blot, (E) Western blot densitometry, and (F) mRNA expression levels of TNF-α, TGF-β, IL-6 and FAS by qRT-PCR. Scale bars = 50 μm. Values are mean ± SEM. $^{*}p < 0.05$, $^{**}p < 0.01$, $^{***}p < 0.001$ versus control (CON) group, $^{\#}p < 0.05$, $^{\#\#}p < 0.01$, $^{\#\#\#}p < 0.001$ versus high-fat diet (HFD) group, $^{\$\$}p < 0.01$, $^{\$\$\$}p < 0.001$ versus high-fat diet containing GS 100 mg/kg body weight (HFD+GS 100 mg/kg) group.

levels of lipid (TC, TG, HDL- and LDL-cholesterol). In our present study, all groups fed with GS showed significant decreases in regards to body weight gain, food and energy efficiency ratios, and the organ relative to the HFD group. The food intake of HFD+GS 500 mg/kg group was decreased in comparison to other groups; we expect this to be attributable to an antisweet property of GS. In addition, GS effectively reduced the serum levels lipid relative to the HFD group. Previous studies have shown that hyperglycemia and insulin resistance are induced by a HFD, and have related glucose homeostasis and insulin resistance to body weight loss and improved serum lipid levels (Choi *et al.*, 2013). GS could help promote body weight loss by controlling serum lipid parameters such as TC, TG, in STZ diabetic or HFD induced models (Potawale *et al.*, 2008; Kishore *et al.*, 2014).

The exact mechanisms of how GS is able to improve these body composition and serum lipid parameters have not yet been revealed. Some researchers have investigated the mechanisms of GS; it may suppress the increase of blood glucose levels by inhibiting glucose uptake in the intestine and increasing the secretion of insulin in the pancreas (Potawale *et al.*, 2008; Kishore *et al.*, 2014). In our study, we confirmed that GS significantly reduced the level of fasting glucose, serum insulin, and HOMA-IR and HbA1c after the consumption of a HFD. Furthermore, the single oral administration of GS showed antidiabetic effects in a postprandial state and this mechanism was based on the inhibition of amylase activity. Amylases are enzymes that break down of disaccharide or oligo to monosaccharides, and the inhibition of an amylase is known to cause a delayed digestion of carbohydrates (Srinivasulu *et al.*, 2016). This decreased activity suggests that GS could decrease the rate of glucose absorption and regulate lipid level.

Adipose tissue is known to be an important site of inflammation, energy homeostasis and for the maintenance of lipid flux (Tanaka *et al.*, 2015; García-Ruiz *et al.*, 2015). Its dysfunction could lead to insulin resistance and NAFLD. Many reports have demonstrated that increased macrophages in adipose tissue are correlated with obesity (Lumeng and Saltiel, 2011; Luo *et al.*, 2015). Here we show that the consumption of a HFD led to an increase in white adipose tissue inflammation and adiposity, however, GS showed significantly reversed results. Forming crown-like structures because of macrophage infiltration in the adipose tissue is known for the main inducer of inflammation, and we confirmed that GS significantly decrease the percentage of F4/80-positive cells per total cells. In addition, when adipocytes are stimulated with toll-like receptors, they activate NF-κB and p38 (Jiang *et al.*, 2011), and we confirmed that GS significantly decreases their protein levels. These results indicated that GS could ameliorate the adipose tissue inflammation induced by a HFD.

Brown adipose tissue is also related to the modulation of energy balance and thermogenesis induction, which are important for body weight maintenance and glucose homeostasis (García-Ruiz *et al.*, 2015). UCP-1 is a key component of thermogenesis and is used as the brown adipocyte-specific gene marker. Several studies showed that HFD increased the thermogenic capacity, which can lead to the maintenance of body weight and the dissipation of excess energy intake. We confirmed that HFD significantly decreased UCP-1 expression in white adipose tissue, but increased in brown adipose tissue relative to the CON group. Protein levels also showed opposite results in white and brown

adipose tissue. This result supports the findings of previous studies, and indicates that HFD acts as stimulus for the activation of brown adipose tissue. White adipose tissue browning induction can also prevent an increase energy waste (García-Ruiz *et al.*, 2015). Our data showed that GS could reverse browning in white adipose tissue.

Furthermore, we investigated the cytokines in white adipose tissue: leptin and adiponectin. Leptin is a key factor in regulating energy intake and expenditure, and it is well known that decreased leptin synthesis is associated with lipolysis (Qureshi and Abrams, 2007; Mopuri *et al.*, 2015). Adiponectin is an adipocyte-specific protein and is well known to regulate insulin sensitivity and glucose homeostasis (Tolman *et al.*, 2007). Our study demonstrated that GS significantly lowered the leptin levels and improved the mRNA expression levels. Taken together, GS could effectively improve adiposity and inflammation in adipose tissue as well as energy homeostasis.

Since NAFLD has also been linked to obesity, we investigated whether GS could improve the liver steatosis induced by a HFD (Tarantino *et al.*, 2010; Luo *et al.*, 2015). GS was found to effectively alleviate the NAS and TG levels in the liver; serum AST and ALT levels were used as markers of liver damage (Strauss *et al.*, 2000; Kim *et al.*, 2016). Sirius red staining and F4/80 IHC of the liver, protein and mRNA levels indicated that GS could effectively improve the NAFLD induced by a HFD.

In conclusion, our data support the acute hyperglycemic effect of GS in the postprandial state, as well as, the existence of a relationship between insulin resistance, and the dysfunction of adipose tissue and the liver induced by a HFD. GS demonstrated preventative effects against HFD-induced metabolic disorders when it was used as a functional dietary supplement in this study. However, further studies are needed to investigate the relationship between its antisweet property and food intake in a pair-wise feeding study in order to investigate the control of food intake and its beneficial effect.

Acknowledgments

This work was supported by BK21 PLUS Program for Creative Veterinary Science Research and Research Institute for Veterinary Science, Seoul National University.

References

Asai, A., P.M. Chou, H.F. Bu, X. Wang, M.S. Rao, A. Jiang, C.J. Didonato and X.D. Tan. Dissociation of hepatic insulin resistance from susceptibility of nonalcoholic fatty liver disease induced by a high-fat and high carbohydrate diet in mice. *Am. J. Physiol. Gastrointest. Liver Physiol.* 306: G496–504, 2014.

Begriche, K., J. Massart, M.A. Robin, F. Bonnet and B. Fromenty. Mitochondrial adaptations and dysfunctions in nonalcoholic fatty liver disease. *Hepatology* 58: 1497–1507, 2013.

Bhutani, K.K., R.B. Birari and K. Kapat. Potential anti-obesity and lipid lowering natural products: A review. *Nat. Prod. Commun.* 2: 331–348, 2007.

Choi, H.K., E.K. Won, Y.P. Jang and SY. Choung. Antiobesity effect of *Codonopsis lanceolata* in high calorie/high-fat-diet-induced obese rats. *Evid. Based Complement Alternat. Med.* 2013: 210297, 2013.

Daisy, P., J. Eliza and K.A. Mohamaed Farook. A novel dihydroxy gymnemic triacetate isolated from *Gymnema sylvestre* possessing normoglycemic and hypolipidemic activity on STZ-induced diabetic rats. *J. Ethnopharmacol.* 126: 339–344, 2009.

Duval, C., U. Thissen, S. Keshtkar, B. Accart, R. Stienstra, MV. Boekschoten, T. Roskams, S. Kersten and M. Müller. Adipose tissue dysfunction signals progression of hepatic steatosis towards nonalcoholic steatohepatitis in C57BL/6 mice. *Diabetes.* 59: 3181–31, 2010.

Gao, M., Y. Ma and D. Liu. High-fat diet-induced adiposity, adipose inflammation, hepatic steatosis and hyperinsulinemia in outbred CD-1 mice. *PLoS One.* 10: e0119784, 2015.

García-Ruiz, E., B. Reynés, R. Díaz-Rúa, E. Ceresi, P. Oliver and A. Palou. The intake of high fat diets induces the acquisition of brown adipocyte gene expression features in white adipose tissue. *Int. J. Obes. (Lond)* 39: 1619–1629, 2015.

Gastaldelli, A., S.A. Harrison, R. Belfort-Aguilar, L.J. Hardies, B. Balas, S. Schenker and K. Cusi. Importance of changes in adipose tissue insulin resistance to histological response during thiazolidinedione treatment of patients with nonalcoholic steatohepatitis. *Hepatology* 50: 1087–1093, 2009.

Jiang, C., A. Qu, T. Matsubara, T. Chanturiya, W. Jou, O. Gavrilova, Y.M. Shah and F.J. Gonzalez. Disruption of hypoxia-inducible factor 1 in adipocytes improves insulin sensitivity and decreases adiposity in high-fat diet fed mice. *Diabetes* 60: 2484–2495, 2011.

Jin, D., X. Yi and X. Mei. Anti-obesity and lipid lowering effects of theaflavins on high fat diet induced obese rats. *J. Funct. Foods* 5: 1142–1150, 2013.

Kim, H.J., S.H. Hong, S.H. Chang, S. Kim, A.Y. Lee, Y. Jang, O. Davaadamdin, K.N. Yu, J.E. Kim and M.H. Cho. Effect of feeding a diet containing *Gymnema sylvestre* extract: Attenuating progression of obesity in C57BL/6J mice. *Asian Pac. J. Trop. Med.* 9: 427–434, 2016.

Kishore, L., N. Kaur and R. Singh. Role of *Gymnema sylvestre* as alternative medicine. *J. Homeop. Ayurv. Med.* 3: 172–180, 2014.

Kosaraju, J., A. Dubala, S. Chinni, R.B. Khatwal, M.N. Satish Kumar and D. Basavan. A molecular connection of *Pterocarpus marsupium*, *Eugenia jambolana* and *Gymnema sylvestre* with dipeptidyl peptidase-4 in the treatment of diabetes. *Pharm. Biol.* 52: 268–271, 2014.

Kumar, V., U. Bhandari, C.D. Tripathi and G. Khanna. Anti-obesity effect of *Gymnema sylvestre* extract on high fat diet-induced obesity in Wistar rats. *Drug Res. (Stuttg).* 63: 625–632, 2013.

Kusum, D. and J. Nimisha. A validated HPLC method for estimation of Gymnemic acids as Deacyl gymnemic acid in various extracts and formulations of *Gymnema sylvestre*. *Int. J. Phytomed.* 6: 165–169, 2014.

Leach, M.J. Gymnema sylvestre for diabetes mellitus: A systematic review. *J. Altern. Complement. Med.* 13: 977–983, 2007.

Li, Q., Z. Liu, J. Huang, G. Luo, Q. Liang, D. Wang, X. Ye, C. Wu, L. Wang and J. Hu. Anti-obesity and hypolipidemic effects of Fuzhuan brick tea water extract in high-fat diet-induced obese rats. *J. Sci. Food Agric.* 93: 1310–1316, 2013.

Lumeng, C.N. and A.R. Saltiel. Inflammatory links between obesity and metabolic disease. *J. Clin. Invest.* 121: 2111–2117, 2011.

Luo, Y., C.M. Burrington, E.C. Graff, J. Zhang, R.L. Judd, P. Suksaranjit, Q. Kaewpoowat, S.K. Davenport, A.M. O'Neill and M.W. Greene. Metabolic phenotype and adipose and liver features in a high-fat Western diet induced mouse model of obesity-linked NAFLD. *Am. J. Physiol. Endocrinol. Metab.* 310: E418–439, 2015.

Mopuri, R., M. Ganjayi, K.S. Banavathy, B.N. Parim and B. Meriga. Evaluation of anti-obesity activities of ethanolic extract of *Terminalia paniculata* bark on high fat diet-induced obese rats. *BMC Complement Altern. Med.* 15: 76, 2015.

Potawale, S.E., VM. Shinde, A. Libi, S. Borad, H. Dhalawat and R.S. Deshmukh. Gymnema sylvestre: A comprehensive review. *Pharmacologyonline Newsletter* 2: 144–157, 2008.

Pothuraju, R., R.K. Sharma, J. Chagalamarri, S. Janqra and K.P. Kumar. A systematic review of Gymnema sylvestre in obesity and diabetes management. *J. Sci. Food Agric.* 94: 834–840, 2013.

Qureshi, K. and G.A. Abrams. Metabolic liver disease of obesity and role of adipose tissue in the pathogenesis of nonalcoholic fatty liver disease. *World J. Gastroenterol.* 13: 3540–3553, 2007.

Reddy, R.M., P.B. Lathan, T. Vijaya and D.S. Rao. The saponin-rich fraction of a *Gymnema sylvestre* R. Br. aqueous leaf extract reduces cafeteria and high-fat diet-induced obesity. *Z. Naturforsch. (C).* 67: 39–46, 2012.

Shanmugasundaram, E.R., G. Rajeswari, K. Baskaran, B.R. Rajesh Kumar, K. Radha Shanmugasundaram and B. Kizar Ahmath. Use of *Gymnema sylvestre* leaf extract in the control of blood glucose in insulin-dependent diabetes mellitus. *J. Ethnopharmacol.* 30: 281–294, 1990.

Shigematsu, N., Asano, M. Shimosakan and M. Okazaki. Effect of administration with the extract of *Gymnema sylvestre* R. Br leaves on lipid metabolism in rats. *Biol. Pharm. Bull.* 24: 713–717, 2001.

Srinivasulu, N., P. Mallaiah, G. Sudhakar, R.B. Sasi Bhusana and D. Sarala. Alpha amylase inhibitory activity and in vitro glucose uptake in psoas muscle and adipose tissue of male wistar rats of leaf methanolic extract of *Achyranthes aspera*. *J. Pharmacogn. Phytochem.* 5: 176–180, 2016.

Strauss, R.S., SE. Barlow and W.H. Dietz. Prevalence of abnormal serum aminotransferase values in overweight and obese adolescents. *J. Pediatr.* 136: 727–733, 2000.

Tanaka, N., S. Takahashi, T. Matsubara, C. Jiang, W. Sakamoto, T. Chanturiya, R. Teng, O. Gavrilova and F.J. Gonzalez. Adipocyte-specific disruption of fat-specific protein 27 causes hepatosteatosis and insulin resistance in high-fat diet-fed mice. *J. Biol. Chem.* 290: 3092–3105, 2015.

Tarantino, G., S. Savastano and A. Colao. Hepatic steatosis, low-grade chronic inflammation and hormone/growth factor/adipokine imbalance. *World J. Gastroenterol.* 16: 4773–4783, 2010.

Tiwari, P., B.N. Mishra and N.S. Sangwan. Phytochemical and pharmacological properties of Gymnema sylvestre: An important medicinal plant. *Biomed Res Int.* 2014: 830285, 2014.

Tolman, K.G., V. Fonseca, A. Dalpiaz and M.H. Tan. Spectrum of liver disease in type 2 diabetes and management of patients with diabetes and liver disease. *Diabetes Care* 30: 734–743, 2007.

van der Heijden, R.A., F. Sheedfar, M.C. Morrison, P.P. Hommelberg, D. Kor, N.J. Kloosterhuis, N. Gruben, S.A. Youssef, A. de Bruin, M.H. Hofker, R. Kleemarnn, D.P. Koonen and P. Heeringa. High-fat diet induced obesity primes inflammation in adipose tissue prior to liver in C57BL/6j mice. *Aging (Albany NY).* 7: 256–268, 2015.

Vermaak, I., A.M. Viljoen and J.H. Hamman. Natural products in anti-obesity therapy. *Nat. Prod. Rep.* 28: 14931533, 2011.

Yu, K.N., H.J. Kim, S. Kim, O. Davaadamdin, A.Y. Lee, S.H. Hong, S.H. Chang, S.J. Choi, S.M. Shim, K. Lee and M.H. Cho. Cigarette smoking condensate disrupts endoplasmic reticulum–golgi network homeostasis through GOLPH3 expression in normal lung epithelial cells. *Nicotine Tob. Res.* 18: 1877–1885, 2016.

Supplementary Figure

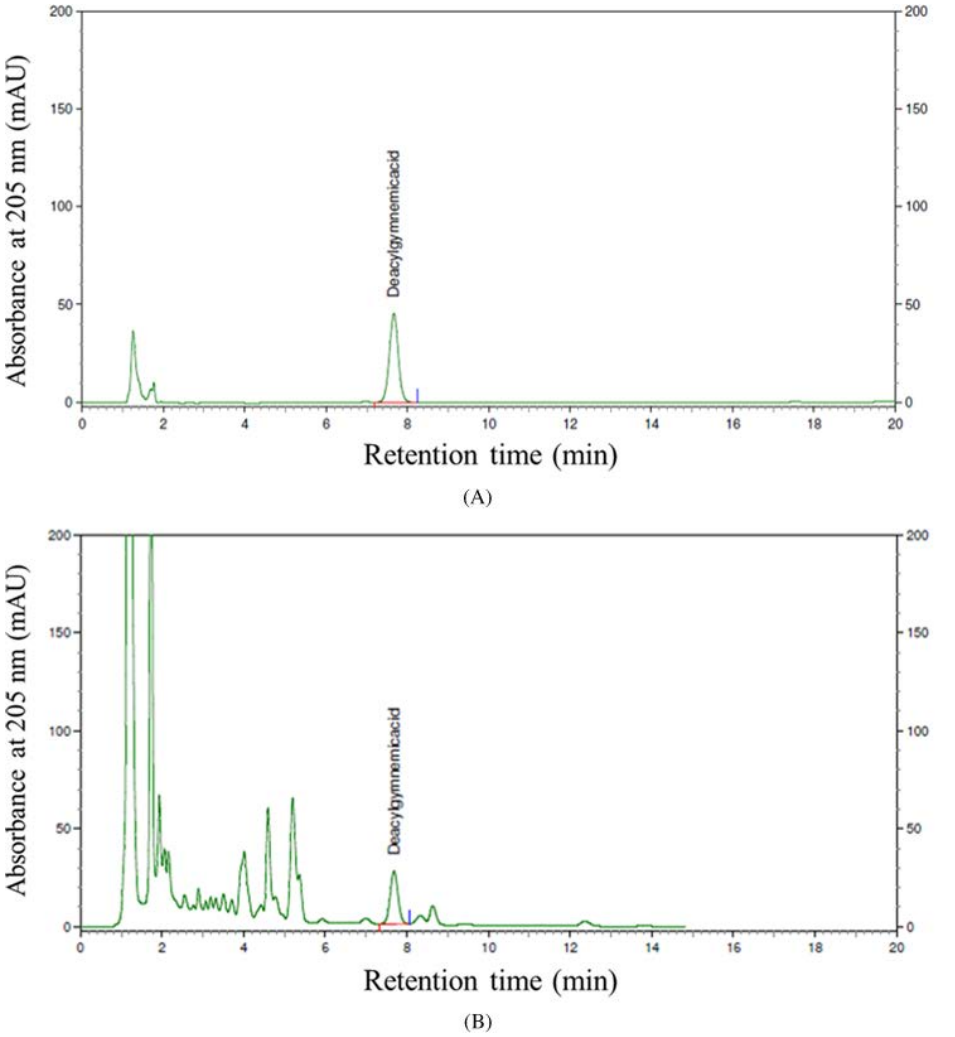

Supplementary Figure 1. HPLC chromatogram of (A) deacyl gymnemic acid and (B) estimation of gymnemic acids as *deacyl gymnemic acid*.

Table S1. Description of *Gymnema Sylvestre* Extract

Physical Profile	
Particle size	80 Mesh: 90%, 40 Mesh: 95%
Loose density	0.30–0.70 g/ml
Bulk density	0.64 g/ml
Product profile	
Identification	To pass by TLC
Loss on drying	3.6%
Residual solvent	<50.00 ppm
Assay	
Gymnemic Acid by HPLC (as Deacylgymnemic acid)	10.2 (% w/w)
Total gymnemic Acid by Gravimetry	25.4 (% w/w)

Table S2. Experimental Diet Composition and Energy Contents

			HFD+GS(mg/kg body weight)		
Macronutrients	**CON**	**HFD**	**100**	**250**	**500**
Carbohydrate (%)	70.00	20.00	20.00	20.00	20.00
Protein (%)	20.00	20.00	20.00	20.00	20.00
Fat (%)	10.00	60.00	60.00	60.00	60.00
Ingredients (g/kg)					
Casein	189.56	258.45	258.11	257.62	256.79
L-Cystine	2.84	3.88	3.87	3.86	3.85
Corn Starch	521.30	—	—	—	—
Maltodextrin	142.17	161.53	161.32	161.01	160.49
Sucrose	—	88.91	88.79	88.62	88.34
Cellulose	47.39	64.61	64.53	64.40	64.20
Soybean Oil	23.70	32.31	32.26	32.20	32.10
Lard	18.96	316.60	316.19	315.58	314.57
Mineral Mix	9.48	12.92	12.91	12.88	12.84
DiCalcium Phosphate	12.32	16.80	16.78	16.75	16.69
Calcium Citrate	5.21	7.11	7.10	7.08	7.06
Potassium Citrate	15.64	21.32	21.29	21.25	21.19
Vitamin Mix	9.48	12.92	12.91	12.88	12.84
Choline Bitartrate	1.90	2.58	2.58	2.58	2.57
Gymnema sylvestre extract	—	—	1.29	3.22	6.42

Table S3. Primer Sequences for qRT-PCR

Name	Forward	Reverse
TNF-α	5′-CACGTCGTAGCAAACCACCAAGTGGA-3′	5′TGGGAGTAGACAAGGTACAACCC-3′
TGF-β	5′-GACCGCAACAACGCCATCTA-3′	5′-GGCGTATCAGTGGGGGTCAG-3′
FAS	5′-GGGACAGGACAAGACAAAAAGGG-3′	5′-AGCCACGAGTGAGTGTACGGGAG-3′
Leptin	5′-ATGTGGTACGGAAGGTGGAG-3′	5′-TGGCTACCTTCGTCTGTGTG-3′
Adiponectin	5′-TGTTGGAATGACAGGAGCTGAA-3′	5′-CACACTGAAGCCTGAGCGATAC-3′
SREBP-1c	5′-TAGAGCATATCCCCCAGGTG-3′	5′-GGTACGGGCCACAAGAAGTA-3′
IL-6	5′-GTCCTTCAGAGAGATACAGAAAC-3′	5′-GCTCCTTAGCCACTCCTT-3′
GAPDH	5′-CGTGCCGCCTGGAGAAACC-3′	5′-TGGAAGAGTGGGAGTTGCTGTTG-3′